



Structural variation of forest edges across Europe

Camille Meeussen, Sanne Govaert, Thomas Vanneste, Kim Calders, Kurt Bollmann, Jörg Brunet, Sara A.O. Cousins, Martin Diekmann, Bente Jessen Graae, Per-Ola Hedwall, et al.

► To cite this version:

Camille Meeussen, Sanne Govaert, Thomas Vanneste, Kim Calders, Kurt Bollmann, et al.. Structural variation of forest edges across Europe. Forest Ecology and Management, 2020, 462, pp.117929. <10.1016/j.foreco.2020.117929>. <hal-02997576>

HAL Id: hal-02997576

<https://hal.science/hal-02997576v1>

Submitted on 10 Nov 2020

HAL is a multi-disciplinary open access archive for the deposit and dissemination of scientific research documents, whether they are published or not. The documents may come from teaching and research institutions in France or abroad, or from public or private research centers.

L'archive ouverte pluridisciplinaire **HAL**, est destinée au dépôt et à la diffusion de documents scientifiques de niveau recherche, publiés ou non, émanant des établissements d'enseignement et de recherche français ou étrangers, des laboratoires publics ou privés.



HAL Authorization

1 **Structural variation of forest edges across Europe**

2 Camille Meeussen^a, Sanne Govaert^a, Thomas Vanneste^a, Kim Calders^b, Kurt Bollmann^c, Jörg
3 Brunet^d, Sara A. O. Cousins^e, Martin Diekmann^f, Bente J. Graae^g, Per-Ola Hedwall^d, Sruthi M.
4 Krishna Moorthy^b, Giovanni Iacopetti^h, Jonathan Lenoirⁱ, Sigrid Lindmo^g, Anna Orczewska^j, Quentin
5 Ponette^k, Jan Plue^e, Federico Selvi^h, Fabien Spicherⁱ, Matteo Tolosano^{a,l}, Hans Verbeeck^b, Kris
6 Verheyen^a, Pieter Vangansbeke^a and Pieter De Frenne^a

7

8 ^aForest and Nature Lab, Department of Environment, Faculty of Bioscience Engineering, Ghent
9 University, Geraardsbergsesteenweg 267, 9090 Melle-Gontrode, Belgium

10 ^bCAVElab – Computational and Applied Vegetation Ecology, Department of Environment, Faculty
11 of Bioscience Engineering, Ghent University, Coupure Links 653, 9000 Ghent, Belgium

12 ^cSwiss Federal Institute for Forest, Snow and Landscape Research WSL, Zürcherstrasse 111, 8903
13 Birmensdorf, Switzerland

14 ^dSouthern Swedish Forest Research Centre, Swedish University of Agricultural Sciences, Box 49,
15 230 53 Alnarp, Sweden

16 ^eBiogeography and Geomatics, Department of Physical Geography, Stockholm University, Svante
17 Arrhenius väg 8, 106 91 Stockholm, Sweden

18 ^fVegetation Ecology and Conservation Biology, Institute of Ecology, FB2, University of Bremen,
19 Leobener Str. 5, 28359 Bremen, Germany

20 ^gDepartment of Biology, Norwegian University of Science and Technology, Høgskoleringen 5, 7491
21 Trondheim, Norway

22 ^hDepartment of Agriculture, Food, Environment and Forestry, University of Florence, P. le Cascine
23 28, 50144 Florence, Italy

24 ⁱUR « Ecologie et Dynamique des Systèmes Anthropisés » (EDYSAN, UMR 7058 CNRS-UPJV),
25 Jules Verne University of Picardie, 1 Rue des Louvels, 80037 Amiens, France

26 ^jDepartment of Ecology, Faculty of Biology and Environmental Protection, University of Silesia,
27 Bankowa 9, 40-007 Katowice, Poland

28 ^kEarth and Life Institute, Université catholique de Louvain, Croix de Sud 2, 1348 Louvain-la-Neuve,
29 Belgium

30 ^lStream Biofilm and Ecosystem Research Laboratory, School of Architecture, Civil and
31 Environmental Engineering, École Polytechnique Fédérale de Lausanne, Bâtiment GR A1 445
32 (Station 2), 1015 Lausanne, Switzerland

33

34 **Corresponding author**

35 camille.meeussen@ugent.be

36 **Abstract**

37 Forest edges are interfaces between forest interiors and adjacent land cover types. They are important
38 elements in the landscape with almost 20 % of the global forest area located within 100 m of the edge.
39 Edges are structurally different from forest interiors, which results in unique edge influences on
40 microclimate, functioning and biodiversity. These edge influences have been studied for multiple
41 decades, yet there is only limited information available on how forest edge structure varies at the
42 continental scale, and which factors drive this potential structural diversity. Here we quantified the
43 structural variation along 45 edge-to-interior transects situated along latitudinal, elevational and
44 management gradients across Europe. We combined state-of-the-art terrestrial laser scanning and
45 conventional forest inventory techniques to investigate how the forest edge structure (e.g. plant area
46 index, stem density, canopy height and foliage height diversity) varies and which factors affect this
47 forest edge structural variability. Macroclimate, management, distance to the forest edge and tree
48 community composition all influenced the forest edge structural variability and interestingly we
49 detected interactive effects of our predictors as well. We found more abrupt edge-to-interior gradients
50 (i.e. steeper slopes) in the plant area index in regularly thinned forests. In addition, latitude, mean
51 annual temperature and humidity all affected edge-to-interior gradients in stem density. We also
52 detected a simultaneous impact of both humidity and management, and humidity and distance to the
53 forest edge, on the canopy height and foliage height diversity. These results contribute to our
54 understanding of how environmental conditions and management shape the forest edge structure. Our
55 findings stress the need for site-specific recommendations on forest edge management instead of
56 generalized recommendations as the macroclimate substantially influences the forest edge structure.
57 Only then, the forest edge microclimate, functioning and biodiversity can be conserved at a local
58 scale.

1. Introduction

The interface between forest and adjacent land is gaining research relevance as it represents a substantial area; almost 20 % of the global forested area is positioned within 100 m of a forest edge (Haddad et al., 2015). The total surface area of forest edges continues to increase as forests are becoming more and more fragmented (Riitters et al., 2016; Taubert et al., 2018). According to Riitters et al. (2016), the loss of forest interiors is at least two times higher than the net loss of forest area, which results in an accumulating number of forest edges.

Forest edges help to preserve the biodiversity in the forest interior from the adverse conditions that predominate outside forest interiors and provide suitable habitat conditions for a variety of both forest specialists and generalist species (Honnay et al., 2002; Melin et al., 2018; Wermelinger et al., 2007; Govaert et al., 2019). Secondly, in addition to biodiversity, also carbon, nutrient and water cycling are altered inside forest edges (Schmidt et al., 2017). In comparison with forest interiors, forest edges are characterized by higher levels of atmospheric nitrogen deposition (Weathers et al., 2001; De Schrijver et al., 2007; Remy et al., 2016) and higher influx of herbicides and fertilizers from adjacent arable lands (Correll, 1991; Kleijn and Snoeiijing, 1997). A third important characteristic of forest edges is that their microclimate is different from the forest interior (Young and Mitchell, 1994; Chen et al., 1995; Saunders et al., 1999; Schmidt et al., 2019). Forest microclimates are increasingly considered in climate-change research and imperative for the conservation of shade-tolerant forest specialists (Lenoir et al., 2017; De Frenne et al., 2019; Zellweger et al., 2019b).

Forest edges are not similar everywhere but differ in their structure, composition and functioning. Together with edge history, orientation, climate and management (Matlack, 1994; Strayer et al., 2003; Esseen et al., 2016), the adjacent, often intensive, land-use management practices will strongly impact the forest edge structure and composition. Species composition itself could further shape the edge structure as trees differ in their architecture and ability to react to the increased light availability near an edge (Mourelle et al., 2001; Niinemets, 2010). For instance, shade-tolerant trees have a higher branching density and a more voluminous crown (Mourelle et al., 2001). Finally, patch contrast, the

85 difference in composition and structure between forest and non-forested land, is another determinant
86 of the forest edge structure (Harper et al., 2005). Patch contrast, and in particular the contrast in
87 canopy height, is related to forest edge characteristics and composition but also to climate, since this
88 affects the productivity. In productive ecosystems (e.g. at lower latitude and elevations), patch
89 contrast in canopy height is expected to be higher (Esseen et al., 2016). Understanding how these
90 factors affect the structure and composition of forest edges is important, as ultimately the structure
91 will modify the edge functioning and habitat availability, making edges significantly different from
92 the forest interiors (Harper et al., 2005).

93 Both the three-dimensional structure as well as the tree species composition of forest edges can be
94 used as descriptors to better capture the biodiversity, nutrient cycling and microclimate in forest
95 edges. Complex edges with structurally diverse vertical layers provide shelter and different food
96 resources for a variety of species (Lindenmayer et al., 2000; Wermelinger et al., 2007). Hence, they
97 may thus act as local hotspots or potential refugia, on a longer term, for biodiversity (Goetz et al.,
98 2007; Zellweger et al., 2017; Melin et al., 2018). In terms of the understorey vegetation, Hamberg et
99 al. (2009) found that side-canopy openness, tree species composition and distance to the forest edge
100 were the main structural metrics affecting the understorey vegetation. Additionally, it has been
101 demonstrated that gradually building up the vertical complexity of forest edges (e.g. fringe, mantle
102 and shrub layer) mitigates the negative effects of atmospheric deposition (Wuyts et al., 2009). Finally,
103 forest edge structure and tree species composition also partly control the microclimatic differences
104 between the exterior and interior condition, and thus the establishment of a typical forest microclimate
105 (Young and Mitchell, 1994; Didham and Lawton, 1999; Davies-Colley et al., 2000; Schmidt et al.,
106 2019). From an open area onwards, gradients in temperature, light, humidity and wind are mediated
107 by the presence of a forest edge leading towards a moderate climate subject to less variability inside
108 the forest (Davies-Colley et al., 2000; Ewers and Banks-Leite, 2013). For example, organisms living
109 under a denser canopy layer experience lower maximum temperatures (Greiser et al., 2018; De Frenne
110 et al., 2019; Zellweger et al., 2019a) and higher minimum temperatures (Chen et al., 1999; Saunders

111 et al., 1999; De Frenne et al., 2019; Zellweger et al., 2019a) than organisms living near edges and in
112 fully open conditions. The main determinants of the forest microclimate are canopy openness and
113 cover (Ehbrecht et al., 2019; Zellweger et al., 2019a). In addition, structural metrics associated with
114 old growth forest (i.e. a tall canopy, vertical heterogeneous structure and high biomass) are known to
115 contribute to a higher buffering capacity (Frey et al., 2016; Kovács et al., 2017).

116 The forest edge provides many ecological processes that are directly associated and beneficial to
117 adjacent land uses and its structure influences the depth and magnitude of the edge influence on
118 ecosystem processes (Harper et al., 2005; Wuyts et al., 2009; Schmidt et al., 2019). Yet, large-scale
119 studies analysing the variation of the structure and tree composition of forest edges are lacking.
120 However, Esseen et al. (2016) studied the variability in forest edge structure across Sweden and
121 detected variation in multiple forest edge structural variables associated with edge origin, land use,
122 climate and tree species composition. Most of the other studies focusing on forest edge structure are
123 often system specific and performed at local scales, covering restricted spatial extents (Cadenasso et
124 al., 2003). To our knowledge, no continental-scale assessment of forest edge structure has been
125 undertaken so far. This is surprising, not only due to their importance, but also due to the high
126 plausibility that forest edges strongly vary in space and time (Schmidt et al., 2017).

127 Moreover, to date, when studying forest edges, most authors have only provided a relatively limited
128 description of the structure (Schmidt et al., 2019) which makes it hard to compare edge influences on
129 forest structure and composition (Harper et al., 2005). The development of new methods such as state-
130 of-the-art 3D terrestrial laser scanning (TLS, also referred to as terrestrial light detection and ranging
131 (LiDAR)) have made it possible to assess the vegetation structure in unprecedented nearly millimetre-
132 level accuracy (van Leeuwen and Nieuwenhuis, 2010; Liang et al., 2016). TLS is also beneficial due
133 to its rapid, objective and automatic documentation and more importantly the possibility to extract
134 non-conventional forest metrics (Dassot et al., 2011; Liang et al., 2016). Doing so, the vertical
135 distribution of plant material can be determined in high detail, which is an important characteristic of
136 the forest and edge structure and a significant driver of microclimate (Wang and Li, 2013; Frey et al.,

2016), habitat availability and biodiversity (Goetz et al., 2007; Melin et al., 2018). Therefore, TLS is increasingly used for inventorying a large number of sites in a comparable way, but very few studies have collected local TLS-data in a replicated design covering a large spatial extent (i.e. continental extent).

Here we quantified structural variation using conventional forest inventory techniques and state-of-the-art terrestrial laser scanning across 45 edge-to-interior transects in deciduous broadleaved forests along latitudinal and elevational gradients across Europe. Our major objective was to study the variation in forest edge structural metrics. We studied how large environmental gradients, driven by temperature and humidity, affected the edge structure (i.e. canopy cover, canopy openness, total basal area, stem density, mean diameter at breast height (DBH), the coefficient of variation of the DBH, plant area index, canopy height, the peak in plant material density and the height of this peak and finally the foliage height diversity). We expected to find structurally different forest edges across Europe, resulting from changes in the macroclimate (light, temperature and precipitation) similar to the global patterns in vegetation structure and composition (Aussenac, 2000; Quesada et al., 2012). A decrease in temperature and/or water availability could limit the productivity and thereby reduce, for instance, stem density, canopy height and the amount of plant material. Yet, even on a smaller spatial scale, the microclimate, could affect the vegetation structure and therefore we assumed to detect a changing forest structure from forest edge to interior. Additionally, we assessed what the effects of forest management were within the different regions via a replicated design covering contrasting management types per site. We assumed that management would shape the forest edge structure on a local scale. For example, intensive management (e.g. intensive thinnings) will reduce canopy cover, stem density and the amount of plant material but will increase the canopy openness. This could negatively affect the forest edge's capacity to reduce the impact of the surrounding land. Finally, we took the influence of tree species composition on the forest edge structure into account. We expected that more shade-tolerant species would form denser edges with a higher plant area index and vegetation cover and a lower canopy openness.

2. Material and methods

2.1 Study design and area

We studied forests along a latitudinal gradient from central Italy (42 °N) to central Norway (63 °N), crossing the sub-Mediterranean, temperate and boreonemoral forest biomes of Europe. This approximately 2300 km wide transect captures macroclimatic variation across Europe (Δ mean annual temperature ~ 13 °C). Along this south-north gradient, nine regions were selected (**Figure A1**): (1) Central Italy, (2) Northern Switzerland, (3) Northern France, (4) Belgium, (5) Southern Poland, (6) Northern Germany, (7) Southern Sweden, (8) Central Sweden and (9) Central Norway.

In three regions, i.e. Norway, Belgium and Italy, the study design was replicated along an elevational gradient covering low, intermediate and high elevational sites to include the climatic variation resulting from elevational differences (21 - 908 m above sea level, m a.s.l.) with an expected Δ temperature ~ 5.76 °C (ICAO, 1993). For the six remaining regions, only lowland transects were studied (between 8 and 450 m a.s.l.).

In all 15 sites (i.e. nine lowland, three intermediate and three high-elevation sites), we collected data in three forest stands with a distinct management type. The first type was always a dense and vertically complex forest with a well-developed shrub layer, since it had not been managed for more than 10 years and in general not thinned for at least three decades. A high basal area and canopy cover characterized this type of forest stands, hereafter always referred to as ‘dense forests’. A second type, ‘intermediate forests’, comprised stands with a lower basal area and canopy cover, resulting from regularly thinning (last time approximately five to 10 years ago). The shrub layer in these stands was sparse or absent. The third management type represented ‘open forests’ with a low basal area and higher canopy openness. These forests were intensively thinned in the recent past (one to four years before sampling). Therefore, these forests were structurally simple with no shrub and subdominant tree layer. The studied forests thus represent a ‘chronosequence’ of forest management types along the typical gradient of a management cycle of managed ancient deciduous forests in Europe.

188 We focused on mesic deciduous forests on loamy soils, in general dominated by oaks (mainly
189 *Quercus robur*, *Quercus petraea* or *Quercus cerris*) because these are hotspots for biodiversity,
190 constituting an ecologically important forest type and represent a substantial portion of the deciduous
191 forests across Europe (Bohn and Neuhäusl, 2000; Brus et al., 2012). Other important tree species
192 were *Fagus sylvatica*, *Betula pubescens*, *Populus tremula*, *Ulmus glabra*, *Alnus incana* and *Carpinus*
193 *betulus*. One up to ten different tree species were present per forest stand. All forests were larger than
194 4 ha, and ancient (that is, continuously forested and not converted to another land use since the oldest
195 available land use maps which is typically at least 150-300 years). We selected the three forest stands
196 that best matched the list of selection criteria after multiple field visits (**Appendix A1**), often with
197 assistance from local forest managers, who had knowledge of the area and the historical land-use.

198 2.2 Edge-to-interior transects

199 In each forest, we studied a 100 m-long edge-to-interior gradient. In total, 45 edge-to-interior transects
200 (15 sites and 3 replicates covering the management types per site, **Table A1**) were established, all
201 starting at a southern forest edge to standardize the edge orientation. The studied edges were bordered
202 by arable land or grassland, as is common in highly fragmented landscapes in Europe, and all plots
203 were at least 100 m away from any other forest edge. Each transect encompassed five 3×3 m² plots
204 (thus resulting in 225 plots), all at a fixed distance perpendicular to the edge according to an
205 exponential pattern. The centre of the first plot was located at a distance of 1.5 m from the outermost
206 line of tree trunks, followed by plots centred at 4.5 m, 12.5 m, 36.5 m and 99.5 m from the forest edge
207 towards the interior. If a forest trail was present, we slightly moved the plot away from the trail to
208 avoid effects on the vegetation structure (this was the case in only six plots and never in the two plots
209 closest to the edge).

210 2.3 Forest structure characterisation

211 The forest structure was quantified between May and July 2018 (leaf-on conditions). Characterisation
212 of the forest structure in each plot was done both via a conventional forest inventory survey and via
213 state-of-the-art TLS.

2.3.1 Conventional forest inventory survey

The species-specific percentage cover of all shrub (1 – 7 m) and tree (> 7 m) species was visually estimated (resolution 1 %) within each 3 × 3 m² quadrat. The total vegetation cover was calculated as the cumulative sum of each of the individual tree and shrub species co-occurring within a given quadrat, thus allowing the total cover to exceed 100 % due to overlap as is common in forests (Zellweger et al., 2019a). Next, the centre of each quadrat served as the centre of a larger circular plot with a radius of 9 m. An ultrasound hypsometer (Vertex IV, Haglöf, Sweden) was used to determine the plot dimensions. In these plots, we measured the diameter at breast height (DBH, 1.3 m) of all trees (with DBH ≥ 7.5 cm) with a caliper via two DBH measurements per stem perpendicular to each other. We then calculated the mean DBH per plot and its coefficient of variation (CV). Further, total basal area and stem density per hectare were calculated at plot level. As part of the first and second circular plots extended beyond the forest edge and measurements stopped at the edge (due to the obvious absence of trees), the total basal area and stem density were recalculated for the fraction of forested area. Finally, canopy openness was determined with a convex spherical densiometer (Baudry et al., 2014). Canopy openness at plot level was calculated as the average of three readings: one in the plot's centre and two at a distance of 4.5 m left and right of the centre (following a line parallel to the forest edge), respectively. In sum, we derived six response variables via the conventional field inventory: total vegetation cover, mean DBH, the CV of the DBH, total basal area, stem density and canopy openness.

2.3.2 Terrestrial laser scanning

At each plot, we carried out a single-scan position TLS using a RIEGL VZ400 (RIEGL Laser Measurement Systems GmbH, Horn, Austria) to map the complex three-dimensional structure of the forest plot. The instrument has a beam divergence of nominally 0.35 mrad and operates in the infrared (wavelength 1550 nm) with a range up to 350 m. The pulse repetition rate at each scan location was 300 kHz, the minimum range was 0.5 m and the angular sampling

resolution was 0.04° . Scanning from one single independent location, instead of processing multiple scanning positions, ensures an objective and holistic observation of forest stand structure while being less time consuming compared to multiple scanning positions (Calders et al., 2014; Seidel et al., 2016). The scanner was mounted on a tripod (1.3 m above the ground) and placed in the centre of each plot, where one upright and one tilted scan (90° from the vertical) were taken. These two scans were co-registered, and their data was merged to one point-cloud making use of matrices calculated in the RISCAN Pro software and six reflective targets placed around each of the plots before scanning. The reflectors were used to link and merge the upright and tilted scan as they represent exactly the same locations in both images. Based on the resulting raw point cloud data, a local plane fit was executed to correct for topographic effects. Two adjustments were made to the method described by Calders et al. (2014). Firstly, for the topography correction with TLS plane fitting, a reduced grid (10 m by 10 m) around the scan position was applied. Herein, the lowest points (i.e. ground points) were selected with a 1 m spatial resolution. Secondly, the iterative reweighted least squares regression, accustomed to weight and thus correct for scanner distance of the ground points, was omitted. After performing a local plane fit, vertical profiles of plant area per volume density ($\text{m}^2 \text{m}^{-3}$) (PAVD) as a function of the height were constructed for each plot from the adjusted point cloud. These profiles were based on the gap fraction or the gap probability that represents the probability of a very narrow beam to miss all scattering elements in the forest and escape through the canopy without being intercepted by foliage or wood. Calculation of the gap probability and subsequently the vertical plant profiles is explained in Calders et al. (2014) and was executed in Python making use of the Pylidar library (<http://www.pylidar.org/en/latest/>). Subsequent calculations to derive the respective variables were done in R (R Core Team, 2019). PAVD-profiles illustrate the plant canopy structure and are often used to study the vertical organisation of plant material from the forest floor to the top of the canopy (Calders et al., 2014). Based on the profiles, we extracted several forest

structural metrics. Firstly, we determined the plant area index (PAI), which is the total area of woody (e.g. branches and stems) and non-woody biomass (i.e. leaves) per unit of surface area. The PAI was determined at plot level as the integral of the PAVD over the canopy height. Secondly, a canopy related structural metric, namely canopy top height was extracted. Canopy top height was based on the 99 % PAVD-percentile to remove atmospheric noise. Consequently, the peak in PAVD or thus the maximum density and its height were derived from the profiles. We also quantified the vertical heterogeneity in plant material along the profile, namely, the foliage height diversity (FHD). The FHD was calculated as the Shannon-Wiener index for diversity, *sensu* MacArthur and MacArthur (1961):

$$FHD = - \sum_i p_i \times \log p_i$$

With p_i representing the proportion of plant material in the i^{th} 1 m vertical layer (i.e. PAVD for a given 1 m vertical layer).

A vertically simple profile will receive a low FHD-value while the value will increase with increasing heterogeneity of the FHD. Lastly, canopy openness was calculated as the average percentage of gap fraction across the angle 5-70°. In total, six TLS-based response variables were extracted: PAI, canopy top height, the peak in PAVD, the height of this peak, FHD and canopy openness.

2.4 Macroclimatic predictor variables

Meteorological data were downloaded from CHELSA (version 1.2, average climatic conditions over the period 1979-2013 at a spatial resolution of 30 arc sec, equivalent to approximately a 0.5 km² resolution at 50 °N) (Karger et al., 2017). We extracted the mean annual temperature (MAT, °C) and the mean total annual precipitation (MAP, mm/year) for each site. Subsequently, we calculated the de Martonne Aridity Index (DMI), a drought index based on the MAP divided by the MAT plus 10 °C (de Martonne, 1926). High values express a high humidity while areas with water stress are characterized by low values.

291 2.5 Data analysis

292 Variation in forest edge structural metrics across Europe was analysed in R (R Core Team, 2019)
293 making use of linear mixed-effect models (Zuur et al., 2009) and the *lmer* function in the R-package
294 *lme4* (Bates et al., 2015). In all models, region and transect nested within region were added as
295 random effect terms (i.e. random intercepts, as $1 \mid \text{region/transect}$ in R syntax) to account for spatial
296 autocorrelation due to the hierarchical structure of the data; three up to nine unique transects were
297 nested within each region and thus tend to be more similar than transects from another region.

298 In a first set of models, the fixed effects were our four design variables (i.e. latitude, elevation,
299 management type and distance to the edge), including all two-way interactions. Finally, also the
300 community-weighted mean shade tolerance of each plot was added to each model as a covariate.

301 At the local scale, both tree species richness and composition differed across the transects and sites
302 and this could affect the forest structure since tree species differ in their architectural characteristics
303 (Mourelle et al., 2001; Niinemets, 2010). To better account for differences in tree species community
304 composition and their effect on the forest structure and to avoid the detection of patterns in edge
305 structure that are only related to tree species identity or forest development stage, the tree community-
306 weighted mean shade tolerance was used as a predictor. The shade tolerance index (Niinemets and
307 Valladares, 2006) ranges between one and five and describes the tolerance of tree and shrub species
308 to grow in the shade. Very shade-intolerant species (e.g. *Betula pubescens*), requiring high levels of
309 light (> 50 %) to grow, receive a low value (minimum 1) while the opposite (maximum 5 for a 2-5 %
310 light availability) is true for very shade-tolerant species (e.g. *Fagus sylvatica*) (Niinemets and
311 Valladares, 2006). Even though shade tolerance is mainly determined on juveniles, the relative
312 ranking amongst co-existing species stays overall very similar for adults (Grubb, 1998; Niinemets
313 and Valladares, 2006). The shade tolerance was calculated at the plot level and was based on all tree
314 species in the plot weighted by their respective cover in the conventional inventory. The equation
315 below summarises our first set of mixed-effect models, whereby x represents the twelve forest
316 structural metrics.

$$\begin{aligned}
x \sim & (\textit{latitude} \times \textit{elevation}) + (\textit{latitude} \times \textit{management type}) + (\textit{latitude} \times \textit{distance to the edge}) \\
& + (\textit{elevation} \times \textit{management type}) + (\textit{elevation} \times \textit{distance to the edge}) \\
& + (\textit{management type} \times \textit{distance to the edge}) + \textit{shade tolerance} + (1|\textit{region/transect})
\end{aligned}$$

320

321 To achieve a more profound understanding of the patterns and their drivers, two additional sets of
322 models were constructed where latitude and elevation were substituted first by the MAT and secondly
323 by the DMI. Each time management type, distance to the edge and the community-weighted mean
324 shade tolerance of the tree layer were retained as fixed effects and region and transect nested within
325 region as random effects. Two-way interactions were allowed between substitutes and design-
326 variables as well as amongst design variables.

327

328 Since the distribution of our plots follows an exponential pattern, the distance to the edge was log-
329 transformed prior to the analyses. All continuous predictor variables were standardized (z-
330 transformation) to allow for a better-standardized comparison of model coefficients. Two response
331 variables, canopy openness derived via TLS and canopy openness derived via the densiometer, had
332 right-skewed distributions and were log transformed prior to the analyses. For each of the above-
333 mentioned combinations of response variables and models, a backward model selection was executed
334 whereby non-significant effects and/or interaction terms were removed using the *step*-function of the
335 R-package *lmerTest* (Kuznetsova et al., 2017). After model selection, restricted maximum likelihood
336 was employed to assess the model parameters and finally, we corrected our *p*-values for multiple
337 comparison testing making use of false discovery rates (FDR). The FDR is the estimated proportion
338 of Type 1 errors or thus the proportion of comparisons that are wrongly called significant (Pike,
339 2011). Throughout the text, we will always refer to the corrected *p*-values but asterisks in all tables
340 indicate original *p*-values. The proportion of the explained variance by the fixed effects only (i.e.
341 marginal R^2) and the combination of fixed and random effects (i.e. conditional R^2) determined the
342 model fit. To better understand how strong variables at the edge differed from those at the interior,
343 the magnitude of edge influence (MEI) was calculated as well. The MEI was estimated as (edge –

344 interior)/ (edge + interior) for all response variables but separately per management type. The
345 resulting value fluctuates between -1 and 1 whereby 0 represents no edge influence (Harper et al.,
346 2005). Finally, potential associations between predictor variables as well as amongst response
347 variables were identified with Pearson correlations.

348 3 Results

349 An overview of the twelve response variables and their mean and standard deviation in each region
350 can be found in **Table 1**. For almost all variables, there was a high variability between and within
351 regions, as indicated by the differences in mean values and standard deviations, respectively. For
352 instance, there were large differences in stem density; in Norway, the average stem density was the
353 highest whereas France had the lowest stem density. The average basal area on the other hand, was
354 highest in Switzerland and Southern Sweden. In Germany, average canopy cover was the highest and
355 canopy openness the lowest whereas the opposite, the lowest canopy cover and highest canopy
356 openness was found in France. Average canopy openness determined with TLS was also the highest
357 in France but lowest in Switzerland and Germany. Variation between regions and between
358 management types were visualised in the PAVD-profiles (vertical plant profiles from which most of
359 our TLS-variables were derived) in **Figure B1** and **Figure 1** as well. Further, between- and within-
360 site variability in the dominant tree and shrub species was found (**Table A1**). Oaks dominated most
361 of the transects but the species differed between regions (e.g. *Quercus cerris* in Italy whereas in
362 Belgium *Quercus petraea* and *Quercus robur* were the most dominant). In Norway, the dominant tree
363 species were *Alnus incana*, *Ulmus glabra* and *Betula pubescens*.

364 Our first set of models, including the four design variables latitude, elevation, management type and
365 distance to the edge in addition to the mean community-weighted shade tolerance of the tree layer
366 (**Table 2**) showed that the forest structure varied strongly with the distance to the edge. Interestingly,
367 in a few cases, these edge-to-interior gradients depended on one of the other design variables; we
368 found significant interactive effects of the distance to the forest edge with latitude, elevation and/or
369 management. For instance, for the PAI and stem density, we found an interaction effect of distance
370 to the forest edge with management and latitude, respectively. Dense forests exhibited an extended
371 and gradual increase in PAI from the edge to the interior, whereas this increase was weaker in open
372 forests ($p = 0.090$) and significantly more abrupt and shorter in intermediate forests ($p = 0.022$, **Table**

2 and Figure 2). This results in a flatter and quicker saturated edge-to-interior gradient for intermediate forests.

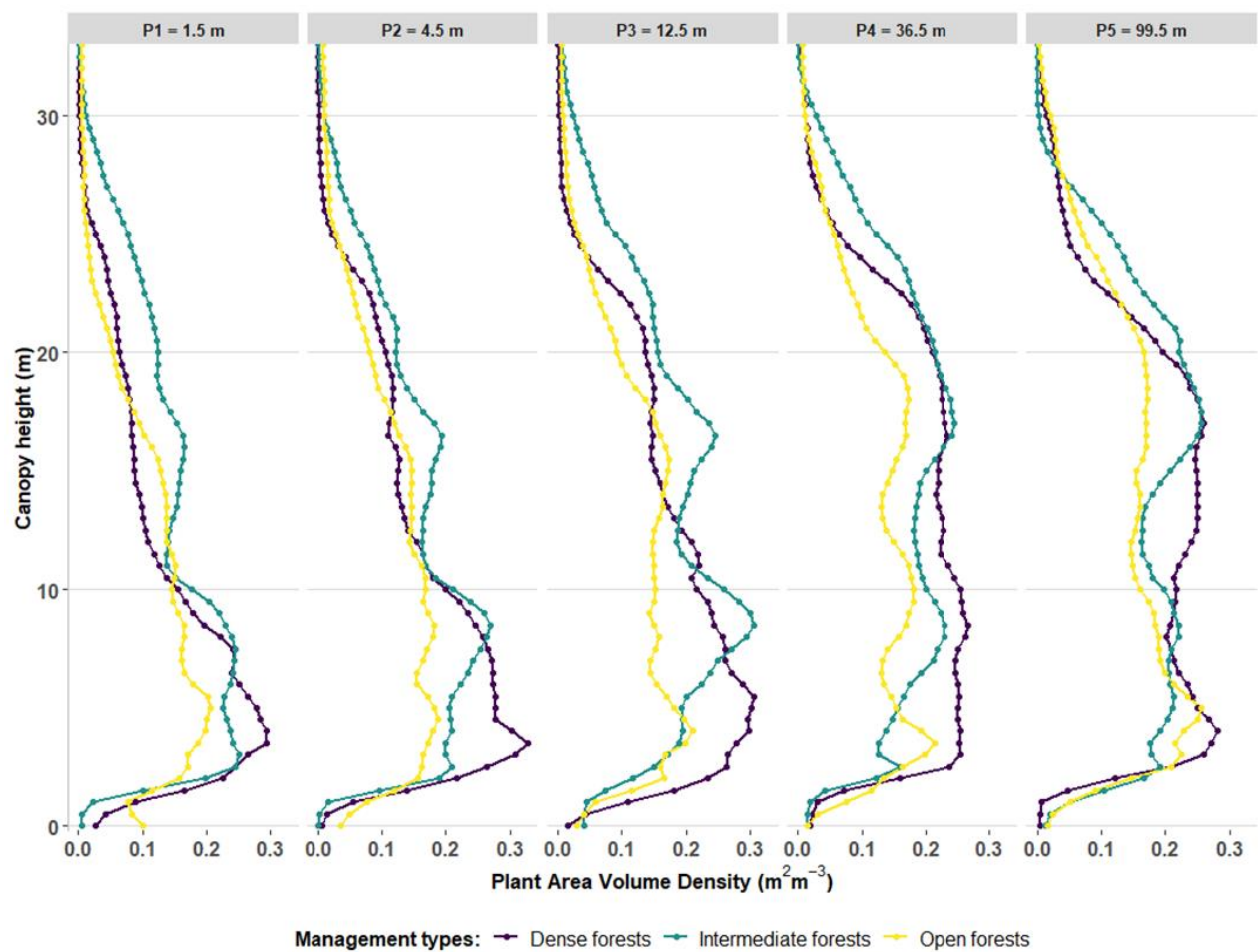
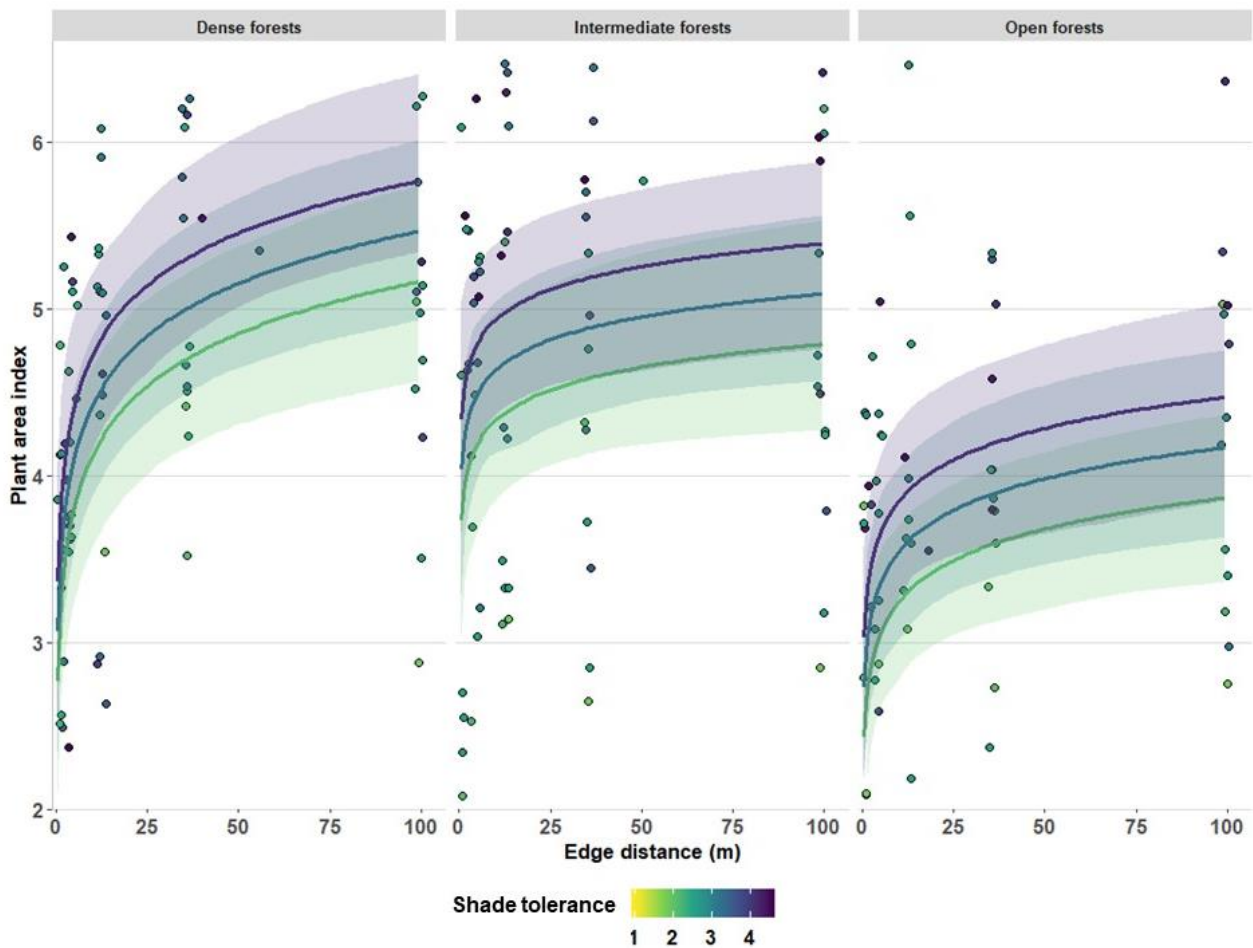


Figure 1: Vertical profiles of plant area per volume density (PAVD) ($\text{m}^2 \text{m}^{-3}$) at different distances from the edge (1.5–99.5 m) for three management types. The profiles were averaged across all regions and elevations ($n = 15$) with management type shown in different colours. **Figure B1**, in the appendix, shows the PAVD-profiles for the nine regions, averaged across all management types and elevations.

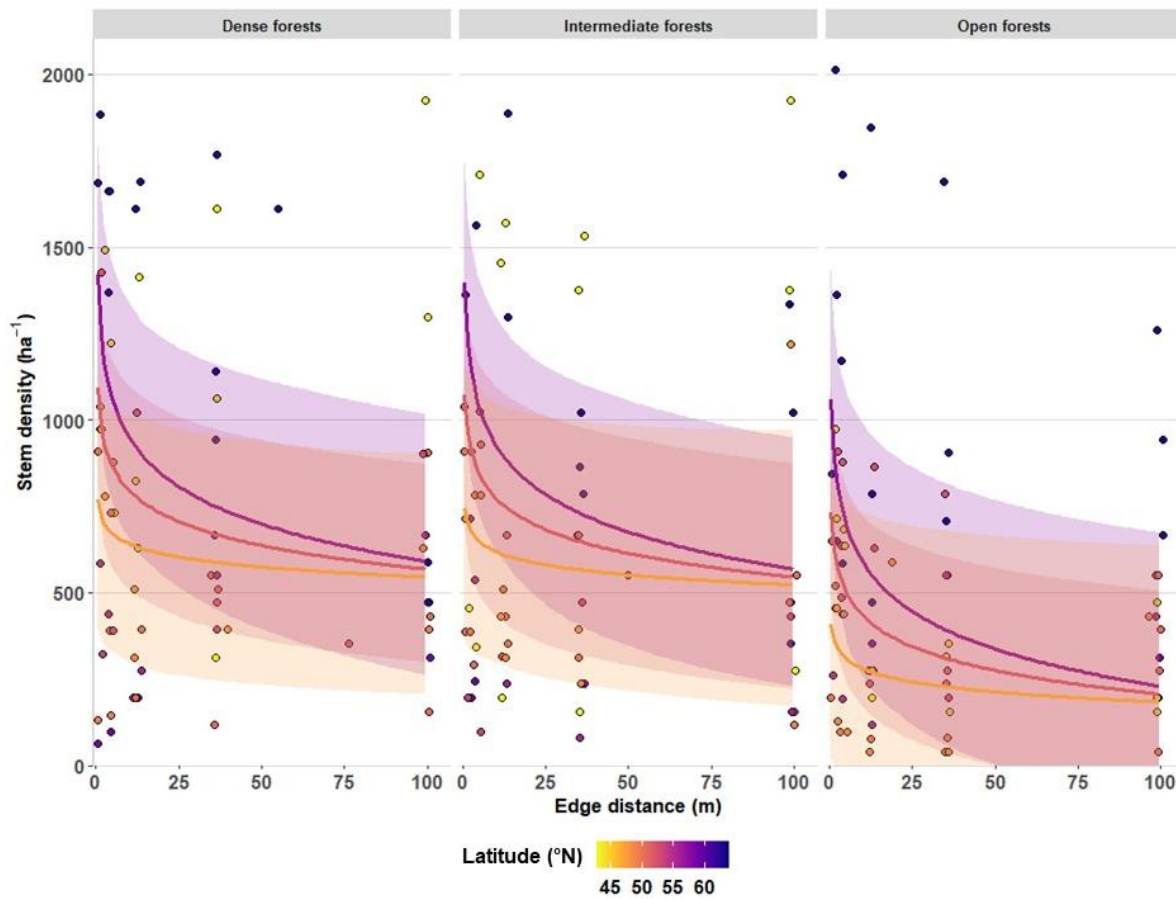
Canopy openness	Estimate				0.15	0.68	-0.45						0.14	0.59
	p-value				0.992	< 0.001 (***)	< 0.001 (***)							
Total basal area	Estimate	3.44	-1.19	-7.76	2.36	-8.30	4.63		2.31				0.27	0.38
	p-value	0.078 (*)	0.777	< 0.001 (***)	0.777	0.078 (*)	0.005 (**)		0.078					
Stem density	Estimate	193.91	87.89	-162.40	-22.79	-361.37		-115.25	-68.19				0.21	0.75
	p-value	0.443	0.443	< 0.001 (***)	1.000	0.055 (*)		< 0.001 (***)	0.015 (**)					
Mean DBH	Estimate		-1.80	-0.94					1.95				0.03	0.50
	p-value		0.960	0.907					0.081 (*)					
Coefficient of variation DBH	Estimate	-0.77		0.45				2.83					0.02	0.33
	p-value	1.000		1.000				0.131 (*)						
Plant area index	Estimate		-0.22	0.65	0.15	-0.92	0.25		-0.12	-0.37	-0.27		0.30	0.66
	p-value		0.190	< 0.001 (***)	0.888	0.029 (*)	0.022 (**)		0.089 (*)	0.022 (**)	0.090			
Canopy height	Estimate		0.28	0.64	0.14	0.46	0.48					-3.04	-0.84	0.10
	p-value		1.000	< 0.001 (***)	1.000	1.000	0.103 (*)					0.089 (*)	1.000	0.91
Maximum PAVD	Estimate		0.01	0.02					-0.01				0.05	0.45
	p-value		1.000	0.001 (***)					0.187 (*)					
Height peak PAVD	Estimate	-1.33	-1.40	2.30	3.86	1.15							0.17	0.34
	p-value	0.142	0.139 (*)	< 0.001 (***)	0.079 (*)	0.945								
Canopy openness	Estimate		0.23	-0.16	0.01	0.87	-0.33		0.11				0.29	0.62
	p-value		0.110	0.007 (**)	1.000	0.010 (**)	< 0.001 (***)		0.079 (*)					
Foliage height diversity	Estimate		-0.08	0.02									0.06	0.84
	p-value		0.220	0.156 (*)										



388

389 **Figure 2:** Plant area index (PAI; mean and 95 % predictions intervals) as a function of the distance to the forest edge (m)
 390 for three management types. The lines show the model predictions of the interaction between distance to the edge and
 391 management. Different colours represent the shade tolerance of the tree layer (values close to one denote low shade
 392 tolerance; values close to five a high shade tolerance). Dots indicate the raw data points; a small amount of noise was
 393 added along the X-axis to improve clarity.

394 Moreover, we detected a decrease in stem density from edge to interior, but this decrease was stronger
 395 at northern latitudes and flattened out towards southern Europe ($p < 0.001$, **Figure 3, Table 2**).
 396 Furthermore, a higher community-weighted mean shade tolerance was found under closed canopies
 397 (densiometer and TLS, $p < 0.001$ for both) and basal area ($p = 0.005$) and the PAI ($p = 0.022$, **Figure**
 398 **2**) were higher when shade tolerance increased (**Table 2**). For canopy openness, we found no edge-
 399 to-interior gradients when assessed by means of the densiometer, whereas these gradients were
 400 significant when quantified with TLS ($p = 0.007$, **Table2**).



401

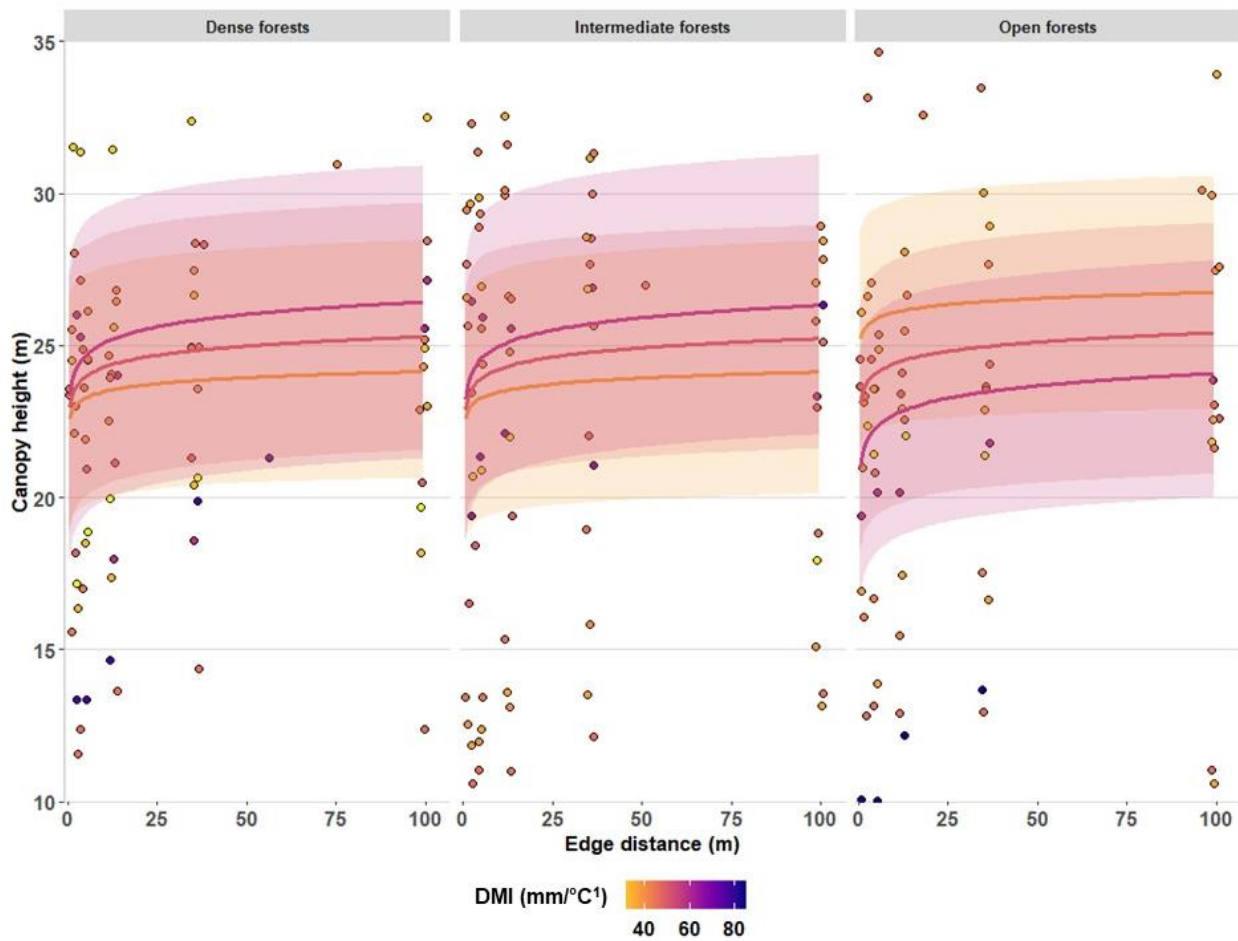
402 **Figure 3:** Stem density (mean and 95 % prediction intervals) as a function of distance to the edge (m) for three
 403 management types. The lines represent the model predictions of the interaction between distance to the edge and latitude;
 404 the colours illustrate the influence of a varying latitude. Elevation was set at its median value when plotting the lines. The
 405 dots show the raw data points; a small amount of noise was added along the X-axis to improve clarity.

406 For our second set of models, where the MAT replaced elevation and latitude to assess macroclimate
 407 temperature effects, we found a significant interaction between MAT and the distance to the forest
 408 edge ($p < 0.001$, **Table B1**) for stem density. As in the first model, there was a strong decrease in
 409 stem density from edge to interior in cold regions whereas the decrease was less distinct in warm
 410 regions (**Figure B2, Table B1**). The results for the PAI were analogous to the first model as well.
 411 Edge-to-interior gradients in PAI were significantly weaker in intermediate forests ($p = 0.019$) in
 412 comparison with dense forests (**Table B1**). Additional significant distance to edge effects were found
 413 for the TLS derived canopy openness ($p = 0.01$) (not for canopy openness determined with the
 414 densiometer), basal area ($p < 0.001$), canopy height ($p < 0.001$), the peak in PAVD ($p = 0.001$) and
 415 the height of the peak in plant material ($p < 0.001$).

416 In a final set of models, we replaced the MAT by the DMI (de Martonne Aridity Index, **Table B2**) to
417 assess macroclimate drought effects. After model selection, DMI was retained as a predictor of the
418 stem density, canopy height and FHD. For the stem density, DMI showed one significant interaction,
419 namely with distance to the edge ($p < 0.001$, **Table B2**); in areas with a higher humidity, stem density
420 decreased more sharply from edge to interior than in regions with a lower DMI (**Figure B2, Table**
421 **B2**). For both canopy height and FHD there were marginally significant interaction effects between
422 DMI and the distance to the forest edge. The increase in canopy height ($p = 0.070$, **Figure 4, Table**
423 **B2**) and FHD ($p = 0.057$, **Figure B3, Table B2**) from forest edge to interior was more pronounced in
424 very humid areas.

425 Besides a marginally significant interaction with distance to the forest edge, an interaction effect
426 between DMI and forest management was found for both canopy height and FHD. Open forests had
427 a higher canopy height and higher foliage height diversity (that is, higher complexity) in drier areas
428 in comparison to intermediate or dense forests. In regions where there was a very high water
429 availability, the opposite was found, namely a higher canopy height and FHD for the dense and
430 intermediate forests ($p = 0.044$ for canopy height, **Figure 4, Table B2** and $p = 0.067$ for FHD, **Figure**
431 **B3, Table B2**). Finally, the PAI and canopy openness were not affected by the DMI. However, for
432 the PAI we found a more or less similar interaction effect of management and distance to the forest
433 edge as in the previous two models (**Table 2, B1 and B2**).

434 Similar results were found for the magnitude of edge influence (MEI). The MEI varied across
435 management types and depended on the studied variable (**Figure B4**). Total basal area and stem
436 density show a high positive MEI, whereas for the PAI the MEI is negative. The average MEI for the
437 PAI was shorter in intermediate than in open or dense forests. For some variables (e.g. total cover,
438 canopy openness determined with the densiometer, mean DBH and FHD), the MEI was close to zero.



439

440 **Figure 4:** Canopy height (mean and 95 % prediction intervals) in function of the distance to the edge (m) for three
 441 management types. The lines show the model predictions of the interaction between water availability (DMI) and
 442 management, as well as between water availability and distance to the edge. Colours illustrate the impact of the DMI.
 443 Shade tolerance was set at its median value when plotting the lines. The dots show the raw data points; a small amount
 444 of noise was added along the X-axis to improve clarity.

445 **4 Discussion**

446 We found that the macroclimate, distance to the edge, forest management and tree species
447 composition all influenced the forest edge structure across Europe. However, we also detected
448 interactive effects of our predictor variables; latitude, mean annual temperature, humidity and
449 management affected edge-to-interior gradients in the forest structure. In addition, we showed that
450 management and humidity simultaneously influenced the forest edge structure.

451 *4.1 The plant area index*

452 The PAI increased towards the forest interior, independent of latitude, MAT or DMI, but was affected
453 by management. The PAI was the lowest in the interiors of open forests (recently thinned forests) and
454 increased towards dense forests. Forest management practices, directly via the removal of stems or
455 indirectly via, for instance tree damage and mortality after management practices (Esseen, 1994;
456 Laurance et al., 1998; Harper et al., 2005; Broadbent et al., 2008), can of course reduce the amount
457 of plant material, followed by a subsequent recovery through increased productivity and regeneration
458 in forest gaps. More interestingly, the interactive effects between management and distance to the
459 forest edge were also significant. The build-up of the biomass towards the interior was more abrupt
460 and quicker saturated in intermediate forests whereas more gradual edges were found both in dense
461 and in open forests. Additionally, the average MEI was also shorter in intermediate forests. A possible
462 explanation for this flatter edge-to-interior gradient in intermediately dense forests can be that there
463 is an enhanced productivity of the remaining trees especially near the forest edge due to a higher
464 resource availability (Smith et al., 2018), weakening the gradual increase in PAI as observed in dense
465 forests or as seen in the first years after harvest (open forests).

466 Tree species composition could further influence these patterns. Our results support a positive effect
467 of shade tolerance on the PAI. Shade-tolerant species (e.g. *Fagus sylvatica*, shade tolerance index of
468 4.56 ± 0.11) can cope with more shade (Niinemets and Valladares, 2006) and have a different crown
469 geometry with a more voluminous crown (Canham et al., 1994; Mourelle et al., 2001) and a higher

470 branching density (Mourelle et al., 2001), creating a more filled and denser canopy. Progressively
471 increasing shade tolerance from edge to interior could therefore create an even smoother and gradual
472 forest edge.

473 *4.2 Stem density and basal area*

474 Higher stem densities at the edge might be due to better regeneration in response to the increased
475 light availability (Palik and Murphy, 1990). Especially noteworthy is that the decreasing trend is
476 stronger in northern than in southern Europe. This may result from the lower solar angles at northern
477 latitudes, which particularly increases light availability at the southern forest edge (Hutchison and
478 Matt, 1977; Harper et al., 2005). In the south, however, the received solar energy per surface unit is
479 higher and differences between edge and interior are less distinct. Here we noticed almost no
480 difference in stem density between edge and interior. Stronger decreases in stem density were also
481 detected in colder regions and regions with a higher water availability due to a strong negative
482 correlation between latitude and MAT and a strong positive correlation between latitude and DMI
483 (**Figure B5**).

484 In response to a lower tree density, we can expect an increased light availability resulting in higher
485 diameter increments (Harrington and Reukema, 1983; Ginn et al., 1991; Aussenac, 2000). Based on
486 the mean DBH or its CV, however, we did not find an impact of management. As a result of the
487 combined impact of a decreasing stem density and a more or less constant DBH, basal area decreased
488 towards the forest interior as previously described by Young and Mitchell (1994).

489 *4.3 Canopy openness*

490 Remarkably, results of canopy openness assessed via TLS and via the densiometer were slightly
491 different. The main difference was that TLS-based canopy openness depended on the distance to the
492 forest edge, whereas no edge impact was found for the densiometer-based openness. Densiometer
493 measurements are visual estimates and are therefore prone to biases related to observer errors,
494 differences amongst operators and a poor resolution (Jennings et al., 1999; Baudry et al., 2014). In

addition, the difference between the two approaches might be caused by scale issues as the scale of the two measurements differed. The densiometer measurements had an intermediate angle of view ($< 60^\circ$) (Baudry et al., 2014) while TLS-derived canopy openness took into account a larger field of view ($5 - 70^\circ$), possibly giving a more detailed representation of the openness and leading to the detection of edge-to-interior-patterns (i.e. a decrease in canopy openness with increasing distance to the forest edge). TLS derived canopy openness might thus be a better tool to study the canopy openness in a more detailed and objective way. Likewise, Seidel et al., (2011) state that especially TLS is recommended when high-resolution canopy information is required.

4.4 Canopy height and the FHD

Canopy height was slightly lower at the forest edge. This could be attributed to an increased wind speed near forest edges, resulting in canopy damage and a reduced canopy height (Laurance et al., 1998; Magnago et al., 2015). Nevertheless, we found that this edge-to-interior gradient in canopy height was affected by gradients in water availability; under conditions of low water availability forests had a lower canopy height likely due to competition for resources. Previous research showed that thinning can reduce canopy height due to a lower competition and the redistribution of nutrients to lateral branches or the trunk (Harrington and Reukema, 1983; Aussenac, 2000). We found such a lower canopy height with management, except in forests with a lower water availability. In drier regions, open, recently managed, forests had a higher canopy height than dense forests. In areas with a higher humidity, the opposite pattern was observed. One possible reason might be that a heavy thinning in a drier area could cause a strong reduction in competition, a drop in total water use and an increased throughfall. Hence, an increase in water availability might benefit the canopy height of the residual trees (Stogsdili et al., 1992; Aussenac, 2000).

Alternatively, canopy heights might be underestimated in dense forests due to shading by a higher number of stems and branches in the lower canopy layers (Watt and Donoghue, 2005; Liang et al., 2016; Muir et al., 2018). This means that the detection of the top of the canopy could be more accurate in drier and open forests, potentially leading to a higher estimated canopy height. Occlusion, the

521 inability to detect remote plant material due to dense vegetation close to the scanner, is especially an
522 issue when using a single scan position and can be reduced by using multiple scanning positions,
523 which is more time consuming and therefore not done in our study (van Leeuwen and Nieuwenhuis,
524 2010; Liang et al., 2016; Wilkes et al., 2017).

525 When tree height increases, the amount of plant material rises and so does the vertical heterogeneity
526 (Müller et al., 2018). We indeed found a strong positive correlation between canopy height and FHD
527 (**Figure B5**) and similar predictors for the FHD and canopy height were retained in our third model.
528 We found that the FHD in open forests was lower than in dense forests in regions with a high water-
529 availability, whereas the opposite was found for areas with a lower humidity. This could be due to a
530 higher canopy in drier and open forests, and thus a higher number of vertical layers in the calculation
531 of the FHD. A potential solution could be to select an equal number of height classes for all canopies
532 instead of working with 1 m bins. However, in our case, this was considered too complicated due to
533 the large range of canopy heights present in the dataset (9.5 up to 39 m) and because, up to now, there
534 is no generally accepted method for the delineation of height classes in the FHD-calculation
535 (McElhinny et al., 2005). Another downside of using the FHD as a metric of complexity is its
536 dependency on the relative amount of plant material in each layer. A high FHD does not always mean
537 a high complexity per se, but could result from a uniform filling of the vertical layers and not of a
538 heterogeneous canopy (Seidel et al., 2016).

539 *4.5 Management and ecological implications*

540 Our results demonstrate that the geographical position and macroclimate affect the forest edge
541 structure. Southern forests and forests in regions with a high MAT could be more susceptible to
542 influences from the non-forest environment (e.g. an increased atmospheric deposition and influx of
543 fertilizers and herbicides but also a larger impact of the macroclimate). They have a lower basal area
544 and lack the sharp increase in stem density towards the edge that is present in northern forests, which
545 helps buffering the forest from the exterior. Similarly, edge influences in drier forests could also be
546 underestimated. This means that in these forests, the spatial extent of edge influences of the adjacent

547 land might be more extended and larger buffer zones are required to protect the microclimate, forest
548 specialists and nutrient cycling in the forest interior. Since macroclimate variation over space
549 influences the forest edge structure in our study, climate change and more frequent extreme heat and
550 drought events (Meehl et al., 2007) might also impact the forest edge structure as predicted by higher
551 MAT and lower DMI-values.

552 Understanding the impact of the above-mentioned factors is important, even though one can hardly
553 control them. Via management and species composition, we can shape the forest edge structure to
554 buffer the interior. Considering species composition, we found a positive impact of shade tolerance
555 on PAI, FHD, canopy height and basal area and a negative impact on canopy openness. Selecting
556 more shade-tolerant species could thus improve the thermal buffering capacity of forests, as old-
557 growth forest characteristics (e.g. high canopy, biomass and complexity) are associated with a higher
558 macroclimatic buffering (Frey et al., 2016; Kovács et al., 2017). This is of vital importance in the era
559 of climate change (De Frenne et al., 2019). However, it is also known that mixing tree species with
560 complementary characteristics generates a dense and filled canopy (Pretzsch, 2014; Jucker et al.,
561 2015; Sercu et al., 2017). If we focus on management, thinning leads to canopy opening, a reduced
562 basal area, stem density and biomass and more abrupt gradients in biomass. These management
563 practices in turn, can increase the impact of edge influences from the adjacent land in the forest
564 interior. If we want to protect the forest interior, dense and gradual forest edges, on the other hand,
565 can be beneficial since they reduce both the magnitude and depth of edge influences (Harper et al.,
566 2005). Gradual edges are, for instance, less susceptible to atmospheric nitrogen deposition (Wuyts et
567 al., 2009) while a dense edge with a high canopy cover is important for the establishment of the forest
568 microclimate and the reduction of maximum temperatures (Zellweger et al., 2019a). On the other
569 hand, an increase in canopy openness, due to the harvest of trees, can locally increase the temperature
570 and the impact of macroclimate warming (Zellweger et al., 2019a).

571 We further show that the impact of management practices in the different regions is not static, but
572 influenced by the time since management (e.g. PAI increases from open to dense forests and edge-

573 to-interior gradients in PAI are modified by the management type). Such dynamics are at present
574 often ignored when studying microclimates or ecosystem functions such as carbon sequestration near
575 edges as most research focusses on static edges (Smith et al., 2018). Not taking into account such a
576 dynamic behaviour could, similarly to disregarding the large-scale variation in forest edge structure,
577 underestimate the impact of the buffering capacity of the forest interior.

578 *4.6 Implications for future research*

579 Even though we sampled in three management types and thereby a large variability in forest
580 complexity and openness, not the whole range of possible forest edge types was sampled. Therefore,
581 for instance, we lack natural and unmanaged edges, which are less abrupt but more complex (Esseen
582 et al., 2016). Extending the range of edge types in addition to a random selection of forest edges could
583 improve our insights on the impact of management on the forest edge structure. Further, since we
584 only investigated deciduous forests generally dominated by oaks, additional research on the impact
585 of macroclimate, management and distance to the forest edge in other forest types could render new
586 information. In coniferous forests, a more abrupt, less variable edge structure is to be expected as
587 their capacity to respond to gaps in the canopy or edge formation is limited in comparison to
588 deciduous trees (Esseen et al., 2016). Therefore, these edges probably receive a higher atmospheric
589 deposition and are less capable of buffering the impact of the macroclimate. Research by Renaud and
590 Rebetez (2009), for instance, already showed that buffering of maximum temperatures is linked to
591 canopy closure and therefore more pronounced in broadleaved and mixed forests than in forests
592 dominated by conifers.

593 The use of TLS in forest inventories is beneficial due to its objectivity and accuracy. Probably, the
594 most important advantage of TLS is the possibility to study metrics nearly impossible to quantify
595 with conventional forest inventory techniques (Dassot et al., 2011; Liang et al., 2016), such as the
596 vertical structural variability. However, this technique is still costly and especially time-consuming.
597 Even when using single-scan TLS, reducing the data acquisition time, the data processing remains
598 time-consuming. Conventional forestry techniques, on the other hand, are easy applicable and require

599 less data processing. Therefore, traditional methods to extract, for instance, stem density and basal
600 area do still have their advantages over TLS. A conventional forestry inventory can thus provide the
601 researcher with a profound basis on the forest structure, though if enhanced or very detailed forest
602 measurements are required (e.g. vertical variability), conventional techniques and TLS can be very
603 complementary.

604 5. Conclusions

605 We studied differences in forest edge structure and their predictors for deciduous oak-dominated
606 forests, subject to different management types along a large latitudinal gradient (2300 km) covering
607 various macroclimatic zones in Europe. Macroclimate, forest management, distance to the forest edge
608 and tree species composition all affected the forest edge structure. We found that edge influence could
609 currently be underestimated in forests at lower latitudes, with a high MAT or lower water availability.
610 Additionally, forest management interventions could negatively affect the edge quality (i.e. lower
611 canopy cover and stem density and a higher canopy openness). This tends to reduce the microclimate
612 buffering capacity of the forest and makes the edge more susceptible to atmospheric depositions. In
613 drier regions, on the other hand, there might be positive effects of an intensive management (i.e.
614 higher canopy height and FHD in open forests). We also found an impact of species composition on
615 the forest edge structure. Selecting species with a higher shade tolerance could further increase the
616 buffering capacity of the edge. Results on edge influences and management guidelines on forest edge
617 structure can thus not be extrapolated or generalised across Europe, since both management and
618 location matter.

619 Further research should focus on other factors that we did not quantify, such as variation in
620 topography, soil properties, nitrogen deposition or biotic interactions with herbivores, with a potential
621 influence on the forest edge structure. If we want to reduce edge influences due to forest
622 fragmentation, more research is necessary to understand this large-scale variability in forest edge
623 structure, to come up with proper region- and context-specific management guidelines.

624 **Acknowledgements**

625 We thank Evy Ampoorter, Haben Blondeel, Filip Ceunen, Kris Ceunen, Robbe De Beelde, Emiel De
626 Lombaerde, Lionel Hertzog, Dries Landuyt, Pierre Lhoir, Audrey Peiffer, Michael Perring, Sanne
627 Van Den Berge, Lotte Van Nevel and Mia Vedel-Sørensen for providing help during the fieldwork
628 campaign.

629 Funding: This work was supported by the European research Council [ERC Starting Grant
630 FORMICA no. 757833, 2018] (<http://www.formica.ugent.be>) and the FWO Scientific research
631 network FLEUR (www.fleur.ugent.be). Thomas Vanneste received funding from the Special
632 Research Fund (BOF) from Ghent University [no. 01N02817].

633 **References**

- 634 Aussenac, G., 2000. Interactions between forest stands and microclimate: Ecophysiological aspects and
 635 consequences for silviculture. *Ann. For. Sci.* 57, 287–301. <https://doi.org/10.1051/forest:2000119>
- 636 Bates, D., Mächler, M., Bolker, B., Walker, S., 2015. Fitting linear mixed-effects models using lme4. *J. Stat.*
 637 *Softw.* 67, 1–48. <https://doi.org/10.18637/jss.v067.i01>
- 638 Baudry, O., Charmetant, C., Collet, C., Ponette, Q., 2014. Estimating light climate in forest with the convex
 639 densiometer: operator effect, geometry and relation to diffuse light. *Eur. J. For. Res.* 133, 101–110.
 640 <https://doi.org/10.1007/s10342-013-0746-6>
- 641 Bohn, U., Neuhäusl, R., 2000. Karte der natürlichen Vegetation Europas, BfN Schriftenvertrieb im
 642 Landwirtschaftsverlag. Bundesamt für Naturschutz, Bonn.
- 643 Broadbent, E.N., Asner, G.P., Keller, M., Knapp, D.E., Oliveira, P.J.C., Silva, J.N., 2008. Forest
 644 fragmentation and edge effects from deforestation and selective logging in the Brazilian Amazon. *Biol.*
 645 *Conserv.* 141, 1745–1757. <https://doi.org/10.1016/J.BIOCON.2008.04.024>
- 646 Brus, D.J., Hengeveld, G.M., Walvoort, D.J.J., Goedhart, P.W., Heidema, A.H., Nabuurs, G.J., Gunia, K.,
 647 2012. Statistical mapping of tree species over Europe. *Eur. J. For. Res.* 131, 145–157.
 648 <https://doi.org/10.1007/s10342-011-0513-5>
- 649 Cadenasso, M.L., Pickett, S.T.A., Weathers, K.C., Jones, C.G., 2003. A framework for a theory of ecological
 650 boundaries. *Bioscience* 53, 750–758. [https://doi.org/10.1641/0006-3568\(2003\)053\[0750:affato\]2.0.co;2](https://doi.org/10.1641/0006-3568(2003)053[0750:affato]2.0.co;2)
- 651 Calders, K., Armston, J., Newnham, G., Herold, M., Goodwin, N., 2014. Implications of sensor
 652 configuration and topography on vertical plant profiles derived from terrestrial LiDAR. *Agric. For.*
 653 *Meteorol.* 194, 104–117. <https://doi.org/10.1016/J.AGRFORMET.2014.03.022>
- 654 Canham, C.D., Finzi, A.C., Pacala, S.W., Burbank, D.H., 1994. Causes and consequences of resource
 655 heterogeneity in forests: interspecific variation in light transmission by canopy trees. *Can. J. For. Res.*
 656 24, 337–349. <https://doi.org/10.1139/x94-046>
- 657 Chen, J., Saunders, S.C., Crow, T.R., Naiman, R.J., Brosnokske, K.D., Mroz, G.D., Brookshire, B.L.,
 658 Franklin, J.F., 1999. Microclimate in forest ecosystem and landscape ecology. *Bioscience* 49, 288–297.

659 <https://doi.org/10.2307/1313612>

660 Chen J., Franklin, J.F., Spies, T.A., 1995. Growing-season microclimatic gradients from clearcut edges into
661 old-growth Douglas-fir forests. *Ecol. Appl.* 5, 74–86. <https://doi.org/10.2307/1942053>

662 Correll, D.L., 1991. Human impact on the functioning of landscape boundaries, in: Holland., M.M., Risser.,
663 P.G., Naiman, R.J. (Eds.), *Ecotones: The Role of Landscape Boundaries in the Management and*
664 *Restoration of Changing Environments*. Springer US, Boston, MA, pp. 90–109.
665 <https://doi.org/10.1007/978-1-4615-9686-8>

666 Dassot, M., Constant, T., Fournier, M., 2011. The use of terrestrial LiDAR technology in forest science:
667 application fields, benefits and challenges. *Ann. For. Sci.* 68, 959–974. [https://doi.org/10.1007/s13595-](https://doi.org/10.1007/s13595-011-0102-2)
668 [011-0102-2](https://doi.org/10.1007/s13595-011-0102-2)

669 Davies-Colley, R.J., Payne, G.W., Van Elswijk, M., 2000. Microclimate gradients across a forest edge. *N. Z.*
670 *J. Ecol.* 24, 111–121.

671 De Frenne, P., Zellweger, F., Rodríguez-Sánchez, F., Scheffers, B.R., Hylander, K., Luoto, M., Vellend, M.,
672 Verheyen, K., Lenoir, J., 2019. Global buffering of temperatures under forest canopies. *Nat. Ecol. Evol.*
673 3, 744–749. <https://doi.org/10.1038/s41559-019-0842-1>

674 de Martonne, E., 1926. L'indice d'aridité. *Bull. Assoc. Geogr. Fr.* 3, 3–5.
675 <https://doi.org/10.3406/bagf.1926.6321>

676 De Schrijver, A., Devlaeminck, R., Mertens, J., Wuyts, K., Hermy, M., Verheyen, K., 2007. On the
677 importance of incorporating forest edge deposition for evaluating exceedance of critical pollutant loads.
678 *Appl. Veg. Sci.* 10, 293–298. <https://doi.org/10.1111/j.1654-109X.2007.tb00529.x>

679 Didham, R.K., Lawton, J.H., 1999. Edge structure determines the magnitude of changes in microclimate and
680 vegetation structure in tropical forest fragments. *Biotropica* 31, 17–30. [https://doi.org/10.1111/j.1744-](https://doi.org/10.1111/j.1744-7429.1999.tb00113.x)
681 [7429.1999.tb00113.x](https://doi.org/10.1111/j.1744-7429.1999.tb00113.x)

682 Ehbrecht, M., Schall, P., Ammer, C., Fischer, M., Seidel, D., 2019. Effects of structural heterogeneity on the
683 diurnal temperature range in temperate forest ecosystems. *For. Ecol. Manage.* 432, 860–867.
684 <https://doi.org/10.1016/J.FORECO.2018.10.008>

685 Esseen, P.-A., 1994. Tree mortality patterns after experimental fragmentation of an old-growth conifer forest.
686 *Biol. Conserv.* 68, 19–28. [https://doi.org/10.1016/0006-3207\(94\)90542-8](https://doi.org/10.1016/0006-3207(94)90542-8)

687 Esseen, P.-A., Hedström Ringvall, A., Harper, K.A., Christensen, P., Svensson, J., 2016. Factors driving
688 structure of natural and anthropogenic forest edges from temperate to boreal ecosystems. *J. Veg. Sci.*
689 27, 482–492. <https://doi.org/10.1111/jvs.12387>

690 Ewers, R.M., Banks-Leite, C., 2013. Fragmentation impairs the microclimate buffering effect of tropical
691 forests. *PLoS One* 8, e58093. <https://doi.org/10.1371/journal.pone.0058093>

692 Frey, S.J.K., Hadley, A.S., Johnson, S.L., Schulze, M., Jones, J.A., Betts, M.G., 2016. Spatial models reveal
693 the microclimatic buffering capacity of old-growth forests. *Sci. Adv.* 2, e1501392.
694 <https://doi.org/10.1126/sciadv.1501392>

695 Ginn, S.E., Seiler, J.R., Cazell, B.H., Kreh, R.E., 1991. Physiological and growth responses of eight-year-old
696 loblolly pine stands to thinning. *For. Sci.* 37, 1030–1040.
697 <https://doi.org/10.1093/forestscience/37.4.1030>

698 Goetz, S., Steinberg, D., Dubayah, R., Blair, B., 2007. Laser remote sensing of canopy habitat heterogeneity
699 as a predictor of bird species richness in an eastern temperate forest, USA. *Remote Sens. Environ.* 108,
700 254–263. <https://doi.org/10.1016/J.RSE.2006.11.016>

701 Govaert, S., Meeussen, C., Vanneste, T., Bollmann, K., Brunet, J., Cousins, S.A.O., Diekmann, M., Graae,
702 B.J., Hedwall, P., Heinken, T., Iacopetti, G., Lenoir, J., Lindmo, S., Orczewska, A., Perring, M.P.,
703 Ponette, Q., Plue, J., Selvi, F., Spicher, F., Tolosano, M., Vermeir, P., Zellweger, F., Verheyen, K.,
704 Vangansbeke, P., De Frenne, P., 2019. Edge influence on understorey plant communities depends on
705 forest management. *J. Veg. Sci.* jvs.12844. <https://doi.org/10.1111/jvs.12844>

706 Greiser, C., Meineri, E., Luoto, M., Ehrlén, J., Hylander, K., 2018. Monthly microclimate models in a
707 managed boreal forest landscape. *Agric. For. Meteorol.* 250–251, 147–158.
708 <https://doi.org/10.1016/J.AGRFORMET.2017.12.252>

709 Grubb, P.J., 1998. A reassessment of the strategies of plants which cope with shortages of resources.
710 *Perspect. Plant Ecol. Evol. Syst.* 1, 3–31. <https://doi.org/10.1078/1433-8319-00049>

711 Haddad, N.M., Brudvig, L.A., Clobert, J., Davies, K.F., Gonzalez, A., Holt, R.D., Lovejoy, T.E., Sexton,
 712 J.O., Austin, M.P., Collins, C.D., Cook, W.M., Damschen, E.I., Ewers, R.M., Foster, B.L., Jenkins,
 713 C.N., King, A.J., Laurance, W.F., Levey, D.J., Margules, C.R., Melbourne, B.A., Nicholls, A.O.,
 714 Orrock, J.L., Song, D.-X., Townshend, J.R., 2015. Habitat fragmentation and its lasting impact on
 715 Earth's ecosystems. *Sci. Adv.* 1, e1500052. <https://doi.org/10.1126/sciadv.1500052>

716 Hamberg, L., Lehvävirta, S., Kotze, D.J., 2009. Forest edge structure as a shaping factor of understorey
 717 vegetation in urban forests in Finland. *For. Ecol. Manage.* 257, 712–722.
 718 <https://doi.org/10.1016/J.FORECO.2008.10.003>

719 Harper, K.A., Macdonald, S.E., Burton, P.J., Chen, J., Broszofsky, K.D., Saunders, S.C., Euskirchen, E.S.,
 720 Roberts, D., Jaiteh, M.S., Esseen, P.-A., 2005. Edge influence on forest structure and composition in
 721 fragmented landscapes. *Conserv. Biol.* 19, 768–782. <https://doi.org/10.1111/j.1523-1739.2005.00045.x>

722 Harrington, C.A., Reukema, D.L., 1983. Initial shock and long-term stand development following thinning in
 723 a Douglas-fir plantation. *For. Sci.* 29, 33–46.

724 Honnay, O., Verheyen, K., Hermy, M., 2002. Permeability of ancient forest edges for weedy plant species
 725 invasion. *For. Ecol. Manage.* 161, 109–122. [https://doi.org/10.1016/S0378-1127\(01\)00490-X](https://doi.org/10.1016/S0378-1127(01)00490-X)

726 Hutchison, B.A., Matt, D.R., 1977. The distribution of solar radiation within a deciduous forest. *Ecol.*
 727 *Monogr.* 47, 185–207. <https://doi.org/10.2307/1942616>

728 International Civil Aviation Organization., 1993. Manual of the ICAO standard atmosphere: extended to 80
 729 kilometres (262 500 feet), 3rd ed. International Civil Aviation Organization, Montreal, Quebec.

730 Jennings, S., Brown, N., Sheil, D., 1999. Assessing forest canopies and understorey illumination: canopy
 731 closure, canopy cover and other measures. *Forestry* 72, 59–74. <https://doi.org/10.1093/forestry/72.1.59>

732 Jucker, T., Bouriaud, O., Coomes, D.A., 2015. Crown plasticity enables trees to optimize canopy packing in
 733 mixed-species forests. *Funct. Ecol.* 29, 1078–1086. <https://doi.org/10.1111/1365-2435.12428>

734 Karger, D.N., Conrad, O., Böhner, J., Kawohl, T., Kreft, H., Soria-Auza, R.W., Zimmermann, N.E., Linder,
 735 H.P., Kessler, M., 2017. Climatologies at high resolution for the earth's land surface areas. *Sci. Data* 4,
 736 170122. <https://doi.org/10.1038/sdata.2017.122>

737 Kleijn, D., Snoeiijing, G.I.J., 1997. Field boundary vegetation and the effects of agrochemical drift: botanical
738 change caused by low levels of herbicide and fertilizer. *J. Appl. Ecol.* 34, 1413–1425.
739 <https://doi.org/10.2307/2405258>

740 Kuznetsova, A., Brockhoff, P.B., Christensen, R.H.B., 2017. lmerTest package: tests in linear mixed effects
741 models. *J. Stat. Softw.* 82, 1–26. <https://doi.org/10.18637/jss.v082.i13>

742 Laurance, W.F., Ferreira, L. V., Merona, J.M.R., Laurance, S.G., 1998. Rain forest fragmentation and the
743 dynamics of Amazon tree communities. *Ecology* 79, 2032–2040. [https://doi.org/10.1890/0012-](https://doi.org/10.1890/0012-9658(1998)079[2032:RFFATD]2.0.CO;2)
744 [9658\(1998\)079\[2032:RFFATD\]2.0.CO;2](https://doi.org/10.1890/0012-9658(1998)079[2032:RFFATD]2.0.CO;2)

745 Lenoir, J., Hattab, T., Pierre, G., 2017. Climatic microrefugia under anthropogenic climate change:
746 implications for species redistribution. *Ecography*. 40, 253–266. <https://doi.org/10.1111/ecog.02788>

747 Liang, X., Kankare, V., Hyypä, J., Wang, Y., Kukko, A., Haggrén, H., Yu, X., Kaartinen, H., Jaakkola, A.,
748 Guan, F., Holopainen, M., Vastaranta, M., 2016. Terrestrial laser scanning in forest inventories. *ISPRS*
749 *J. Photogramm. Remote Sens.* 115, 63–77. <https://doi.org/10.1016/J.ISPRSJPRS.2016.01.006>

750 Lindenmayer, D.B., Margules, C.R., Botkin, D.B., 2000. Indicators of biodiversity for ecologically
751 sustainable forest management. *Conserv. Biol.* 14, 941–950. [https://doi.org/10.1046/j.1523-](https://doi.org/10.1046/j.1523-1739.2000.98533.x)
752 [1739.2000.98533.x](https://doi.org/10.1046/j.1523-1739.2000.98533.x)

753 MacArthur, R.H., MacArthur, J.W., 1961. On bird species diversity. *Ecology* 42, 594–598.
754 <https://doi.org/10.2307/1932254>

755 Magnago, L.F.S., Rocha, M.F., Meyer, L., Martins, S.V., Meira-Neto, J.A.A., 2015. Microclimatic
756 conditions at forest edges have significant impacts on vegetation structure in large Atlantic forest
757 fragments. *Biodivers. Conserv.* 24, 2305–2318. <https://doi.org/10.1007/s10531-015-0961-1>

758 Matlack, G.R., 1994. Vegetation dynamics of the forest edge - Trends in space and successional Time. *J.*
759 *Ecol.* 82, 113. <https://doi.org/10.2307/2261391>

760 McElhinny, C., Gibbons, P., Brack, C., Bauhus, J., 2005. Forest and woodland stand structural complexity:
761 Its definition and measurement. *For. Ecol. Manage.* 218, 1–24.
762 <https://doi.org/10.1016/J.FORECO.2005.08.034>

763 Meehl, G.A., Stocker, T.F., Collins, W.D., Friedlingstein, P., Gaye, T., Gregory, J.M., Kitoh, A., Knutti, R.,
764 Murphy, J.M., Noda, A., Raper, S.C.B., Watterson, I.G., Weaver, A.J., Zhao, Z.C., 2007. Global
765 climate projections, in: Solomon, S., Qin, D., Manning, M., Chen, Z., Marquis, M., Averyt, K.B.,
766 Tignor, M., Miller, H.L. (Eds.), *Climate Change 2007: The Physical Science Basis*. Cambridge
767 University Press, Cambridge, United Kingdom and New York, NY, USA, pp. 747–845.

768 Melin, M., Hinsley, S.A., Broughton, R.K., Bellamy, P., Hill, R.A., 2018. Living on the edge: utilising lidar
769 data to assess the importance of vegetation structure for avian diversity in fragmented woodlands and
770 their edges. *Landsc. Ecol.* 33, 895–910. <https://doi.org/10.1007/s10980-018-0639-7>

771 Mourelle, C., Kellman, M., Kwon, L., 2001. Light occlusion at forest edges: an analysis of tree architectural
772 characteristics. *For. Ecol. Manage.* 154, 179–192. [https://doi.org/10.1016/S0378-1127\(00\)00624-1](https://doi.org/10.1016/S0378-1127(00)00624-1)

773 Muir, J., Phinn, S., Eyre, T., Scarth, P., 2018. Measuring plot scale woodland structure using terrestrial laser
774 scanning. *Remote Sens. Ecol. Conserv.* 4, 320–338. <https://doi.org/10.1002/rse2.82>

775 Müller, J., Brandl, R., Brändle, M., Förster, B., de Araujo, B.C., Gossner, M.M., Ladas, A., Wagner, M.,
776 Maraun, M., Schall, P., Schmidt, S., Heurich, M., Thorn, S., Seibold, S., 2018. LiDAR-derived canopy
777 structure supports the more-individuals hypothesis for arthropod diversity in temperate forests. *Oikos*
778 127, 814–824. <https://doi.org/10.1111/oik.04972>

779 Niinemets, Ü., 2010. A review of light interception in plant stands from leaf to canopy in different plant
780 functional types and in species with varying shade tolerance. *Ecol. Res.* 25, 693–714.
781 <https://doi.org/10.1007/s11284-010-0712-4>

782 Niinemets, Ü., Valladares, F., 2006. Tolerance to shade, drought, and waterlogging of temperate northern
783 hemisphere trees and shrubs. *Ecol. Monogr.* 76, 521–547. [https://doi.org/10.1890/0012-9615\(2006\)076\[0521:TTSDAW\]2.0.CO;2](https://doi.org/10.1890/0012-9615(2006)076[0521:TTSDAW]2.0.CO;2)

785 Palik, B.J., Murphy, P.G., 1990. Disturbance versus edge effects in sugar-maple/beech forest fragments. *For.*
786 *Ecol. Manage.* 32, 187–202. [https://doi.org/10.1016/0378-1127\(90\)90170-G](https://doi.org/10.1016/0378-1127(90)90170-G)

787 Pike, N., 2011. Using false discovery rates for multiple comparisons in ecology and evolution. *Methods*
788 *Ecol. Evol.* 2, 278–282. <https://doi.org/10.1111/j.2041-210X.2010.00061.x>

789 Pretzsch, H., 2014. Canopy space filling and tree crown morphology in mixed-species stands compared with
790 monocultures. *For. Ecol. Manage.* 327, 251–264. <https://doi.org/10.1016/J.FORECO.2014.04.027>

791 Quesada, C.A., Phillips, O.L., Schwarz, M., Czimczik, C.I., Baker, T.R., Patiño, S., Fyllas, N.M., Hodnett,
792 M.G., Herrera, R., Almeida, S., Alvarez Dávila, E., Arneth, A., Arroyo, L., Chao, K.J., Dezzeo, N.,
793 Erwin, T., di Fiore, A., Higuchi, N., Honorio Coronado, E., Jimenez, E.M., Killeen, T., Lezama, A.T.,
794 Lloyd, G., López-González, G., Luizão, F.J., Malhi, Y., Monteagudo, A., Neill, D.A., Núñez Vargas,
795 P., Paiva, R., Peacock, J., Peñuela, M.C., Peña Cruz, A., Pitman, N., Priante Filho, N., Prieto, A.,
796 Ramírez, H., Rudas, A., Salomão, R., Santos, A.J.B., Schmerler, J., Silva, N., Silveira, M., Vásquez, R.,
797 Vieira, I., Terborgh, J., Lloyd, J., 2012. Basin-wide variations in Amazon forest structure and function
798 are mediated by both soils and climate. *Biogeosciences* 9, 2203–2246. [https://doi.org/10.5194/bg-9-](https://doi.org/10.5194/bg-9-2203-2012)
799 2203-2012

800 R Core Team (2019). R: A language and environment for statistical computing. R Foundation
801 for Statistical Computing, Vienna, Austria. URL <https://www.R-project.org/>.

802 Remy, E., Wuyts, K., Boeckx, P., Ginzburg, S., Gundersen, P., Demey, A., Van Den Bulcke, J., Van Acker,
803 J., Verheyen, K., 2016. Strong gradients in nitrogen and carbon stocks at temperate forest edges. *For.*
804 *Ecol. Manage.* 376, 45–58. <https://doi.org/10.1016/J.FORECO.2016.05.040>

805 Renaud, V., Rebetez, M., 2009. Comparison between open-site and below-canopy climatic conditions in
806 Switzerland during the exceptionally hot summer of 2003. *Agric. For. Meteorol.* 149, 873–880.
807 <https://doi.org/10.1016/j.agrformet.2008.11.006>

808 Riitters, K., Wickham, J., Costanza, J.K., Vogt, P., 2016. A global evaluation of forest interior area dynamics
809 using tree cover data from 2000 to 2012. *Landsc. Ecol.* 31, 137–148. [https://doi.org/10.1007/s10980-](https://doi.org/10.1007/s10980-015-0270-9)
810 015-0270-9

811 Saunders, S.C., Chen, J., Drummer, T.D., Crow, T.R., 1999. Modeling temperature gradients across edges
812 over time in a managed landscape. *For. Ecol. Manage.* 117, 17–31. [https://doi.org/10.1016/S0378-](https://doi.org/10.1016/S0378-1127(98)00468-X)
813 1127(98)00468-X

814 Schmidt, M., Jochheim, H., Kersebaum, K.-C., Lischeid, G., Nendel, C., 2017. Gradients of microclimate,
815 carbon and nitrogen in transition zones of fragmented landscapes – a review. *Agric. For. Meteorol.* 232,

816 659–671. <https://doi.org/10.1016/J.AGRFORMET.2016.10.022>

817 Schmidt, M., Lischeid, G., Nendel, C., 2019. Microclimate and matter dynamics in transition zones of forest
818 to arable land. *Agric. For. Meteorol.* 268, 1–10. <https://doi.org/10.1016/J.AGRFORMET.2019.01.001>

819 Seidel, D., Ehbrecht, M., Puettmann, K., 2016. Assessing different components of three-dimensional forest
820 structure with single-scan terrestrial laser scanning: A case study. *For. Ecol. Manage.* 381, 196–208.
821 <https://doi.org/10.1016/J.FORECO.2016.09.036>

822 Seidel, D., Fleck, S., Leuschner, C., Hammett, T., 2011. Review of ground-based methods to measure the
823 distribution of biomass in forest canopies. *Ann. For. Sci.* 68, 225–244. [https://doi.org/10.1007/s13595-](https://doi.org/10.1007/s13595-011-0040-z)
824 [011-0040-z](https://doi.org/10.1007/s13595-011-0040-z)

825 Sercu, B.K., Baeten, L., van Coillie, F., Martel, A., Lens, L., Verheyen, K., Bonte, D., 2017. How tree
826 species identity and diversity affect light transmittance to the understory in mature temperate forests.
827 *Ecol. Evol.* 7, 10861–10870. <https://doi.org/10.1002/ece3.3528>

828 Smith, I.A., Hutyra, L.R., Reinmann, A.B., Marrs, J.K., Thompson, J.R., 2018. Piecing together the
829 fragments: elucidating edge effects on forest carbon dynamics. *Front. Ecol. Environ.* 16, 213–221.
830 <https://doi.org/10.1002/fee.1793>

831 Stogsdili, W.R., Wittwer, R.F., Hennessey, T.C., Dougherty, P.M., 1992. Water use in thinned loblolly pine
832 plantations. *For. Ecol. Manage.* 50, 233–245. [https://doi.org/10.1016/0378-1127\(92\)90338-A](https://doi.org/10.1016/0378-1127(92)90338-A)

833 Strayer, D.L., Power, M.E., Fagan, W.F., Pickett, S.T.A., Belnap, J., 2003. A classification of ecological
834 boundaries. *Bioscience* 53, 723–729. [https://doi.org/10.1641/0006-3568\(2003\)053\[0723:acoeb\]2.0.co;2](https://doi.org/10.1641/0006-3568(2003)053[0723:acoeb]2.0.co;2)

835 Taubert, F., Fischer, R., Groeneveld, J., Lehmann, S., Müller, M.S., Rödig, E., Wiegand, T., Huth, A., 2018.
836 Global patterns of tropical forest fragmentation. *Nature* 554, 519–522.
837 <https://doi.org/10.1038/nature25508>

838 van Leeuwen, M., Nieuwenhuis, M., 2010. Retrieval of forest structural parameters using LiDAR remote
839 sensing. *Eur. J. For. Res.* 129, 749–770. <https://doi.org/10.1007/s10342-010-0381-4>

840 Wang, Q., Li, P., 2013. Canopy vertical heterogeneity plays a critical role in reflectance simulation. *Agric.*
841 *For. Meteorol.* 169, 111–121. <https://doi.org/10.1016/J.AGRFORMET.2012.10.004>

842 Watt, P.J., Donoghue, D.N.M., 2005. Measuring forest structure with terrestrial laser scanning. *Int. J.*
843 *Remote Sens.* 26, 1437–1446. <https://doi.org/10.1080/01431160512331337961>

844 Weathers, K.C., Cadenasso, M.L., Pickett, S.T.A., 2001. Forest edges as nutrient and pollutant concentrators:
845 potential synergisms between fragmentation, forest canopies, and the atmosphere. *Conserv. Biol.* 15,
846 1506–1514. <https://doi.org/10.1046/j.1523-1739.2001.01090.x>

847 Wermelinger, B., Flückiger, P.F., Obrist, M.K., Duelli, P., 2007. Horizontal and vertical distribution of
848 saproxylic beetles (Col., Buprestidae, Cerambycidae, Scolytinae) across sections of forest edges. *J.*
849 *Appl. Entomol.* 131, 104–114. <https://doi.org/10.1111/j.1439-0418.2006.01128.x>

850 Wilkes, P., Lau, A., Disney, M., Calders, K., Burt, A., Gonzalez de Tanago, J., Bartholomeus, H., Brede, B.,
851 Herold, M., 2017. Data acquisition considerations for Terrestrial Laser Scanning of forest plots.
852 *Remote Sens. Environ.* 196, 140–153. <https://doi.org/10.1016/J.RSE.2017.04.030>

853 Wuyts, K., De Schrijver, A., Vermeiren, F., Verheyen, K., 2009. Gradual forest edges can mitigate edge
854 effects on throughfall deposition if their size and shape are well considered. *For. Ecol. Manage.* 257,
855 679–687. <https://doi.org/10.1016/J.FORECO.2008.09.045>

856 Young, A., Mitchell, N., 1994. Microclimate and vegetation edge effects in a fragmented podocarp-broadleaf
857 forest in New Zealand. *Biol. Conserv.* 67, 63–72. [https://doi.org/10.1016/0006-3207\(94\)90010-8](https://doi.org/10.1016/0006-3207(94)90010-8)

858 Zellweger, F., Coomes, D., Lenoir, J., Depauw, L., Maes, S.L., Wulf, M., Kirby, K.J., Brunet, J., Kopecký,
859 M., Máliš, F., Schmidt, W., Heinrichs, S., den Ouden, J., Jaroszewicz, B., Buyse, G., Spicher, F.,
860 Verheyen, K., De Frenne, P., 2019a. Seasonal drivers of understorey temperature buffering in
861 temperate deciduous forests across Europe. *Glob. Ecol. Biogeogr.* 28, 1774–1786.
862 <https://doi.org/10.1111/geb.12991>

863 Zellweger, F., De Frenne, P., Lenoir, J., Rocchini, D., Coomes, D., 2019b. Advances in microclimate
864 ecology arising from remote sensing. *Trends Ecol. Evol.* 34, 327–341.
865 <https://doi.org/10.1016/j.tree.2018.12.012>

866 Zellweger, F., Roth, T., Bugmann, H., Bollmann, K., 2017. Beta diversity of plants, birds and butterflies is
867 closely associated with climate and habitat structure. *Glob. Ecol. Biogeogr.* 26, 898–906.

868 <https://doi.org/10.1111/geb.12598>

869 Zuur, A., Ieno, E., Walker, N., Saveliev, A., Smith, G., 2009. Mixed effects modelling for nested data, in:

870 Zuur, A.F., Ieno, E.N., Walker, N.J., Saveliev, A.A., Smith, G.M. (Eds.), *Mixed Effects Models and*

871 *Extensions in Ecology* with R. Springer, New York, NY, USA, pp. 101–142.

872